Evaluation of core beta effects on pedestal MHD stability in ITER and consequences for energy confinement

W. Oosterbeek[1], T. Weyens[2], A. Loarte[2], G.T.A. Huijsmans[1,3], F.J. Artola[2,4], A. Polevoi[2], S.H Kim[2]

[1] *Eindhoven University of Technology, Eindhoven, The Netherlands* — [2] *ITER Organization, 13067 St. Paul Lez Durance, France* — [3] *CEA, IRFM, 13108 St. Paul Lez Durance, France* — [4] *Aix-Marseille Université, CNRS, PIIM UMR 7345, 13397 Marseille, France*

Abstract

The maximum stable pedestal pressure has been shown to increase with core pressure and in combination with profile stiffness this can lead to a positive feedback mechanism. However, the effect is shown to saturate for high β in ASDEX-Upgrade [1]. This paper investigates whether this effect appears in ITER scenarios, using ideal MHD numerical codes HELENA and MISHKA for different ITER scenarios from inductive 7.5-15 MA plasmas to steady-state scenarios at 10 MA. No pedestal pressure saturation is found for inductive scenarios; on the contrary for the 10MA steady-state scenario the pedestal pressure is the same for a wide range of total β and is limited by low n kink-peeling modes. Finally, a comparison of the achievable pressure for various levels of core profile stiffness is made with the IPB98(y,2) scaling law.

Introduction

To achieve the ITER fusion production goals it is essential to achieve high energy confinement plasmas (H-mode). Ideal MHD studies of the pedestal stability have shown that the maximum stable pedestal pressure increases with more peaked core pressure profiles due to the Shafranov shift [1]. On the other hand, because of profile stiffness a higher pedestal pressure results in a larger core pressure and higher plasma energy; i.e. a positive feedback mechanism. This effect is shown to have a saturation limit in some cases (e.g. ASDEX-Upgrade [1]), so that extrapolations from current devices, such as JET, [2] may not necessarily be applicable to ITER.

Model

In order to describe this core-edge feedback mechanism, the plasma poloidal beta, β_{tot}, is split into two components: the poloidal pedestal beta, β_{ped} which considers the pedestal, and the poloidal core beta, β_{core} for the core plasma. In this paper we investigate the relation between β_{ped} and β_{tot}, which is assumed to be a power law dependence:

$$\beta_{ped} \propto \beta_{tot}^{\alpha}. \tag{1}$$

The stiffness of the core pressure profile is represented by a another power law, in which the ratio of core and pedestal is related to the input power:

$$\frac{\beta_{core}}{\beta_{ped}} \propto P_{in}^{\delta} \tag{2}$$

with P_{in} the input power and δ a measure for the stiffness. Finally, the relation

$$\beta_{tot} \propto P_{in}^{\gamma} \tag{3}$$

determines the energy confinement scaling with power that can be compared with the IPB98(y,2) scaling law, for which $\gamma = 0.31$ [3]. We determine the parameter α by ideal pedestal MHD stability analysis and then we can evaluate γ for various stifness coefficients δ in a self-consistent form and compare to the ITER scaling law value.

The edge MHD stability analysis performed with MISHKA has been carried out for a range of self-consistent plasma equilibria generated with HELENA in which the bootstrap current has been evaluated according to [4] and the pedestal width (in normalized poloidal flux coordinates) has been assumed to be either constant or to scale as $\Delta_{\psi} \propto \sqrt{\beta_{ped}}$ [5]. The reference pedestal width has been evaluated by application of the model in [6] to ITER plasmas. Our studies have been performed for the flat-top phase of three ITER scenarios (15MA/5.3T Q=10, 10MA/5.3T Q = 5 steady-state and 7.5MA/2.65T half current-half field H-mode scenarios) modelled with ASTRA and CORSICA. MHD stabilty is only evaluated for $s = \sqrt{\psi} \geq 0.5$ as the focus of our study is on the plasma edge.

Results

Figure 1 summarizes the results of the analysis both for constant pedestal width for the 15 MA/5.3 T Q = 10 and the 10 MA/5.3 T steady-state plasma. The stability diagram shows a high β_N limit for both scenarios which corresponds to infernal modes in the core plasma. β_{ped} is limited by external modes which depend on the plasma scenario. For the Q =10 scenario these are the usual peeling-balooning modes with n = 20-30. On the contrary, the steady-state scenario pedestal pressure is limited by low n = 2-4 kink-peeling modes. This difference also modifies the dependence of β_{ped} on β_N which is gradual for the Q = 10 plasma while it is weakly dependent on β_N for wide ranges in this parameter for the steady-state plasma, except at very high β_N values, because of the low n of the instabilities.

The steady state 10 MA case has a much higher stability limit for β_{ped} than the Q = 10 case. This is the result of the lower plasma current and the fact that the stability limit is dictated by kink-peeling modes which scales as $I_p \times B_t$ instead of I_p^2 for ballooning modes.

The points of the upper boundary of stability diagrams have been fitted according to equation 1 to obtain the values of α considering only H-mode conditions ($\beta_N \geq 1.5$ for Q = 10). The results of these fits are shown in figure 2 for the three plasmas studied both considering a constant and varying pedestal width. The 15 MA/5.3 T and 7.5 MA/2.65 T plasmas show similar trends, as expected from balooning stability being dominant, with an increasing β_{ped} with total poloidal β_{tot}. There is no saturation even for β_{tot} values well beyond those required for the achievement of the the Q = 10 goal in ITER at 15 MA ($\beta_{tot} = 0.6 - 0.7$). The values of α (also given in figure 2) for constant pedestal width are much lower than for varying pedestal width showing

(a) 15MA/5.3T   (b) 10MA/5.3T
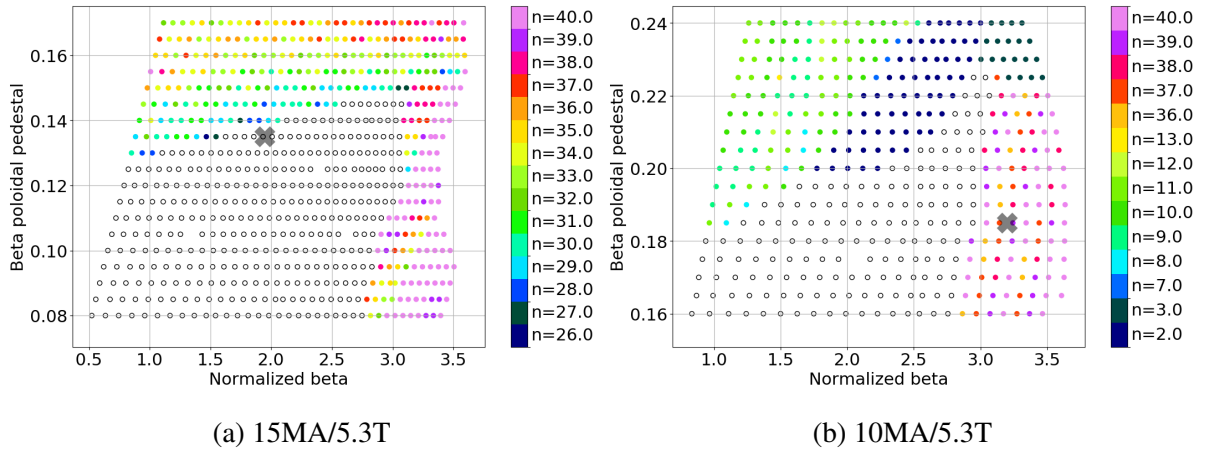
Figure 1: Edge MHD stability diagram characterized by β_{ped} and β_N for the 15MA/5.3T (left) and 10MA/5.3T (right) plasmas with constant pedestal width. Each point represents a different pressure profile for which stability is calculated for toroidal mode numbers n=[2,40]. The most unstable mode is plotted by color with open circles being stable cases. The reference cases, from ASTRA-CORSICA simulations, are indicated by the black cross.

that the positive feedback between core and edge is increased with the widening of the pedestal at higher pressures. For the 10 MA steady-state case the use of a power law is less suitable due to the different nature of the MHD limit stability. Despite this, the results in 1 show that for this case the results are weakly dependent on the changes of the pedestal width with β_{ped}. In particular for the steady-state Q = 5 reference operating the positive feedback is only significant for $\beta_{tot} > 1.2$ for both cases, which is close to the ITER operational point for this scenario.

The values found for α in these ITER plasmas can be compared to experimental values. From [2], values for α in JET plasmas can be evaluated ($\alpha = 0.41, 0.62$ and 0.79), depending on wall material (C vs. W/Be) and plasma shapes. The case closest to the ITER studies for 15 MA and 7.5 MA plasmas corresponds to the JET high triangularity with the carbon wall; this is also most likely to be the condition in which JET edge stability resembles most that of ITER with high pedestal pressure and high bootstrap current achievable with low gas fuelling.

By assuming values for stiffness, the data from figure 2 can be used to find a value for γ from equation 3. This is done for the 15MA case with varying pedestal width in figure 3. Stiffness values of $\delta = [0.1, 2.0]$ are taken, which then gives a relation between δ and γ:

$$\gamma = 1.18\delta. \tag{4}$$

$\gamma = 0.31$ corresponding to the IPB98(y,2) scaling law requires a stiffness of $\delta = 0.26$ according to our modelling.

Summary

We have applied ideal MHD numerical codes HELENA for equilibrium and MISHKA for edge stability analysis to evaluate self-consistently the MHD stability of a range of ITER plas-
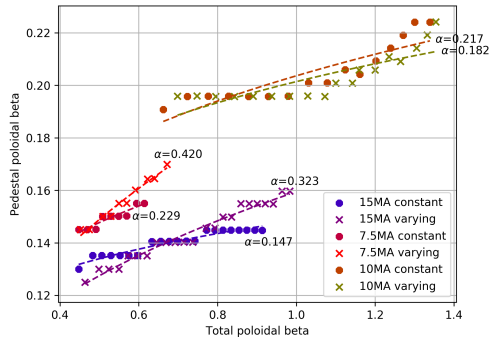
Figure 2: Highest stable β_{ped} values as a function of β_{tot} and corresponding fits for the three ITER plasmas studies, for both constant pedestal width and a pedestal width changing according to the EPED model
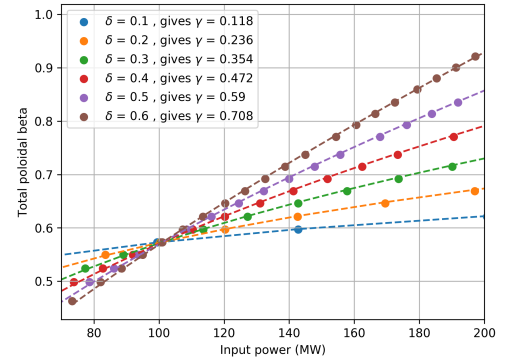
Figure 3: Predicted β_{tot} versus input power for the 15MA plasma with varying pedestal width and β_{ped} limited by edge stability for a range of stiffness parameter δ and resulting energy confinement scaling (γ from equation 3).

mas in terms of the achievable β_{ped} versus β_{tot}. For the 15MA and 7.5 MA plasmas we find that β_{ped} is limited by peeling-balooning modes and increases with β_{tot} according to a power law, whose exponent depends on pedestal width assumptions up to $\beta_{tot} \approx 1$. For the 10 MA steady-state plasmas β_{ped} is limited by low n kin-peeling modes and depends weakly on β_{tot} up to the reference $\beta_{tot} \approx 1.2$. An estimate of the power degradation of energy confinement for a range of core stiffnes parameters for 15 MA plasmas has been provided.

Disclaimer: The views and opinions expressed herein do not necessarily reflect those of the ITER Organization. ITER is the Nuclear Facility INB no. 174.

References

[1] Wolfrum, E., et al. "Impact of wall materials and seeding gases on the pedestal and on core plasma performance", Nuclear Materials and Energy 12 (2017) 18.

[2] Challis, Clive D., et al. "Improved confinement in JET high Îš plasmas with an ITER-like wall." Nuclear Fusion 55.5 (2015): 053031.

[3] ITER Physics Expert Group on Confinement and Transport et al 1999 Nucl. Fusion 39 2175

[4] Sauter, Olivier, Clemente Angioni, and Y. R. Lin-Liu. "Neoclassical conductivity and bootstrap current formulas for general axisymmetric equilibria and arbitrary collisionality regime." Physics of Plasmas 6.7 (1999): 2834-2839.

[5] Leonard, A. W., et al. "Influence of global beta, shape, and rotation on the H-mode pedestal structure in DIII-D." Physics of Plasmas 15.5 (2008): 056114.

[6] Snyder, P. B., et al. "A first-principles predictive model of the pedestal height and width: development, testing and ITER optimization with the EPED model." Nuclear Fusion 51.10 (2011): 103016.